



## Technical note: AI-Track-tive: automated fission track recognition using computer vision (Artificial Intelligence)

Simon Nachtergaele<sup>1</sup>, Johan De Grave<sup>1</sup>

<sup>1</sup>Laboratory for Mineralogy and Petrology, Department of Geology, Ghent University, Ghent, 9000, Belgium

5 *Correspondence to:* Simon Nachtergaele (Simon.Nachtergaele@UGent.be)

### Abstract

Artificial intelligence techniques such as deep neural networks and computer vision are developed for fission track recognition and included in a computer program for the first time. These deep neural networks use the Yolov3 object detection algorithm, which is currently one of the most powerful and fastest object recognition algorithms. These deep neural networks can be used in new software called “AI-Track-tive”. The developed program successfully finds most of the fission tracks in the microscope images, however, the user still needs to supervise the automatic counting. The success rates of the automatic recognition range from 70% to 100% depending on the areal track densities in apatite and (muscovite) external detector. The success rate generally decreases for images with high areal track densities, because overlapping tracks are less easily recognizable for computer vision techniques.

10

### 15 Introduction

Fission track dating is a low-temperature geochronological dating technique applicable on several minerals (mainly apatite and zircon) and glass, and was first developed by Fleischer et al. (1975). Since the discovery of the potential of apatite fission track dating for reconstructing thermal histories (Gleadow et al., 1986), apatite fission track dating has been utilized in order to reconstruct thermal histories of basement rocks and apatite-bearing sedimentary rocks (e.g. Malusà and Fitzgerald (2019); Wagner and Van den haute, (1992)). Anno 2020, more than 200 scientific papers with apatite fission track dating results are published every year. Hence, apatite fission track dating currently is a widely applied technique in tectonic and other studies. Fission track dating techniques are labour-intensive and are highly dependent on accurate and consequent track counting using optical microscopy. Automation of the track identification process and counting could decrease the analysis time. Several attempts have been undertaken in order to develop automatic counting techniques (Belloni et al., 2000; Gold et al., 1984; Kumar, 2015; Petford et al., 1993). The most successful attempt by the Melbourne Thermochronology Group in collaboration with Autoscan Systems Pty was the first to provide an automatic fission track counting system in combination with Zeiss microscopes. The currently only available automatic fission track recognition software package is called FastTracks. It is based on the patented technology of “coincidence mapping” (Gleadow et al., 2009). This procedure includes capturing microscopy images with both reflected and transmitted light. After applying a threshold to both images, a binary image is obtained. Fission tracks are automatically recognized where the binary image of the transmitted light source and reflected light source coincide

20

25

30



(Gleadow et al., 2009). Recently, potential improvements for discriminating overlapping fission tracks were also proposed (de Siqueira et al., 2019).

Despite promising initial tests and agreement between the manually and automatically counted fission track samples reported in Gleadow et al. (2009), challenges remain for the track detection strategy (Enkelmann et al., 2012). The automatic track  
35 detection technique from Gleadow et al. (2009) incorporated in FastTracks (Autoscan) does not work well in the case of (1)  
internal reflections (Gleadow et al., 2009), (2) surface relief (Gleadow et al., 2009), (3) over- or underexposed images  
(Gleadow et al., 2009), (4) shallow-dipping tracks (Gleadow et al., 2009) and (5) very short tracks with very short tails. More  
complex tests of the automatic counting software (FastTracks) undertaken by two analysts from University of Tübingen  
(Germany) showed that automatic counting without manually reviewing leads to severely inaccurate and dispersed counting  
40 results which are less time-efficient than manual counting using the “sandwich technique” (Enkelmann et al., 2012).

This paper presents a new approach for automatic detection of fission tracks in both apatite and muscovite. Normally, fission  
tracks are detected using segmentation of the image into a binary image (Belloni et al., 2000; Gleadow et al., 2009; Gold et  
al., 1984; Petford et al., 1993). Here, in our approach, segmentation strategies are abandoned and replaced by the development  
of computer vision capable of detecting the fission tracks in the mineral. It will be shown later in this paper that artificial  
45 intelligence techniques such as computer vision can be a solution for the labour-intensive manual counting, as already  
recognized by Kumar (2015). Below, it will be shown that a custom-trained deep neural network can detect almost all tracks  
in apatite and muscovite external detectors. This new solution for apatite fission track dating is currently available as an  
executable program (.exe) with the name “AI-Track-tive”. The deep neural networks for apatite and mica are also available to  
the scientific community.

## 50 **1 Methods**

### **1.1 System requirements**

AI-Track-tive uses two custom-trained deep neural networks based on training data of high-quality output microscope images.  
Using these, unanalyzed images can be analyzed automatically after which it is possible to apply manual corrections. Although  
it is tested on output from a Nikon TRACKFlow system (Van Ranst et al., 2020), AI-Track-tive is platform-independent. The  
55 only required input are .jpg images with an appropriate size (for example 804x804px). AI-Track-tive contains a graphical user  
interface (GUI) from which it is easy to choose the specific images and appropriate analysis settings.

### **1.2 Development**

This program utilizes a self-trained fission track recognition deep neural network (Darknet 53) from the Yolov3 object  
detection algorithm (Redmon et al., 2016; Redmon and Farhadi, 2018). This deep neural network is used as an object detection  
60 tool which can be trained for several objects. The deep neural network presented in this paper is trained on only one “class”  
(semi-tracks). Two deep neural networks were trained specifically for semi-tracks in apatite and in mica. They were both



trained on 15 images for apatite and 25 images for mica on 1000x magnification. AI-Track-tive has been developed in Python 3.8 (Van Rossum and Drake Jr, 1995) using several Python modules, such as OpenCV (Bradski, 2000) and Tkinter (Lundh, 1999).

## 65 2 Results

### 2.1 AI-Track-tive: a new program for automated fission track counting

The result of the unique strategy for automated fission track identification is embedded in the “AI-Track-tive” program. It is an interactive program useful for analysing several types of samples, such as (1) an apatite and external detector couple, (2) Uranium-doped glass-covering mica and (3) apatite (Figure 1). The user can import a split z-stack in AI-Track-tive after which  
70 it will automatically find the best focussed image for both apatite and its external detector. The user can either choose for a user-defined polygonal or a circular window in which AI-Track-tive will search for tracks (Figure 1). Due to the very rapid Yolov3 algorithm (Redmon et al., 2016; Redmon and Farhadi, 2018), automatic track recognition is performed almost instantaneously. The result of the track recognition is an image in which every detected fission track is indicated with a rectangle. Every rectangle located for more than half its surface inside the polygon (or region of interest) is counted. Track  
75 detection is not 100% successful for every image. Therefore, manually reviewing is necessary. Tracks can be manually added or removed using the computer mouse buttons. These will be displayed immediately in a different colour on the microscope image. The manually adjusted image is saved as a .png file at the end of the manual reviewing process. Track counting results are exported in .csv files together with all useful information. Hence, performing your own zeta-calibration (Hurford and Green, 1983) or GQR calibration (Jonckheere, 2003) is possible.

### 80 2.2 Success rate of track recognition software

A series of analyses were undertaken in order to evaluate the success rate of the fission track identification in apatite and mica. Several samples with varying areal fission track densities were analysed for apatite (Table 1) and muscovite (Table 2). Small and large apatite grains with varying degrees of Uranium distribution were analysed. Also, less transparent apatite grains with under- and overexposed parts were analysed in order to test the effect of different levels of light exposure on track recognition.  
85 The results of these experiments are listed in Table 1 and Table 2.

#### 2.2.1 Fission track recognition in apatite

The track recognition results on three (100 µm on 100 µm) photos of Durango apatite can be observed in Figure 2. Panel A and B show a polygon in which fission tracks can be counted. Panel C shows the feature for using a circular counting window (useful for LAFT). In panel A of Figure 2, it can be observed that the object detection model finds most of the fission tracks.  
90 Also in panel A of Figure 2, six fission tracks were not found automatically but were also added manually (visible in yellow) using the program. These six fission tracks were not easily recognisable due to overlap with other tracks or they were located



95 at the edge of the photo. Panel B shows an image of a low-quality apatite grain in which a custom-drawn polygonal graticule was used. Panel C shows a Durango apatite photo analyzed using a circular window of 80 $\mu$ m diameter. Panel A and B yield a success rate of 79% and 73%, respectively. Panel C shows an example of a success rate of 100%. Panel B and C also show that the success of the track recognition is not influenced by the brightness of the image. Based on these three examples from Figure 2 it appears that track detection success rate decreases with increasing track density.

### 2.2.2 Fission track recognition in mica

100 The result of fission track recognition in mica is illustrated with one example from a mica attached to a Uranium-doped glass (Figure 3). For this image it was chosen not to use a polygon or graticule. Here, a square of 100  $\mu$ m on 100  $\mu$ m was used to determine the induced areal track density, which is the entire field of view. Figure 3 shows that 55 tracks were automatically detected (in blue) and 4 were manually added (in green). The resulting induced areal track density equals  $5.9 * 10^5 tr/cm^2$  for this single image. In this case, the program detected 93% of the tracks automatically and only 7% of the tracks were not detected, hence, needed to be added manually by the user. These “missed” tracks are in most cases tracks that are either overlapping or barely visible.

### 105 2.3 Analysis time

Two experiments were undertaken in which fission tracks were counted in both apatite and external detector. The results of these experiments are summarized in Table 3 and compared to previous results using FastTracks reported in Enkelmann et al. (2012). For our time analysis experiment, 25 coordinates in a pre-annealed Durango sample (A-DUR) and its external mica detector were analysed by the first author. Selecting and imaging 25 locations in the Durango sample and its external detector took 25-35 min using TRACKFlow (Van Ranst et al., 2020). Counting fission tracks in 25 locations in an annealed Durango sample and its external detector (including manual reviewing) using AI-Track-tive took 30 minutes in total. It is expected that fission track counting would take some more time for samples with track densities higher than ( $\sim 4 * 10^5 tr/cm^2$ ) (Table 1).

## 3 Discussion

### 3.1 Success rate of automatic track recognition

115 The success rate of automatic track recognition has been tested for several ( $\sim 20$ ) different images of apatite and external detector (mica) images. The automatic track recognition results show that the computer vision strategy is (currently) not detecting all semi-tracks in apatite (Table 1) and mica (Table 2). Hence, manual reviewing the results and indicating the “missed” tracks is highly recommended. The success rate of both the apatite and mica fission track recognition is compared to the areal track densities in two scatter plots shown in Figure 4. The upper limit of  $10^7$  tracks/cm<sup>2</sup> was defined as the upper limit for fission track identification using optical microscopy (Wagner, 1978). The lower limit of  $10^5$  tracks/cm<sup>2</sup> was chosen

120



arbitrarily based on the fact that apatite fission track samples in most studies have track densities within the range of  $10^5$  to  $10^7$  tracks/cm<sup>2</sup>. For track densities lower than the arbitrarily set limit of  $10^5$  tracks/cm<sup>2</sup>, it is still possible to do fission track dating but it is more time-consuming with respect to sample scanning and image acquisition (i.e. finding a statistical adequate number of countable tracks in large surface areas and/or high number of individual apatite grains).

125 The two scatter plots of Figure 4 show that the success rate of the automated fission track recognition always remains higher than 70%. This means that the worst case scenario is that the analyst needs to manually select 30% of the fission tracks. The negative slope of the linear regression models in both panels of Figure 4 indicate that the success rate decreases exponentially with increasing areal track densities. This negative slope is observed in both scatter plots and a linear model has been fit through the data points. However, for mica the slope appears to be less steep. The explanation for the negative slope is quite  
130 obvious and relates to the number of coinciding semi-tracks that drastically increase with increasing track densities. Coinciding semi-tracks are difficult to detect for both humans and computers. Therefore, the trained deep neural networks were trained on images (Table 1) in which the track densities were high and sometimes hard to identify.

### 3.2 Current state and outlook

With the development of AI-Track-tive it was possible to successfully introduce artificial intelligence techniques (i.e. computer  
135 vision) into fission track dating. The program presented here performs significantly faster as compared to other automatic fission track recognition software such as TrackWorks from Autoscan systems (Table 3). With the current success rates of the program, we think already a significant gain is to be made. However, manually reviewing the automatic track recognition results is still (and will perhaps always be) necessary. In the near future it seems likely that computer power and artificial intelligence techniques will inevitably improve. Therefore, smarter deep neural networks with higher success rates will likely  
140 be developed in the future. These new deep neural networks will be able to be used in AI-Track-tive.

## 4 Conclusions

In this paper we present a program (“AI-Track-tive”) that uses computer vision for conducting fission track analysis.

AI-Track-tive is:

- innovative because it uses artificial intelligence (deep neural networks) in order to detect fission tracks automatically.
- 145 - capable of successfully finding and identifying 70-100% of the fission tracks depending on the areal track densities of the sample. The fraction of unrecognised tracks can be manually added in an interactive window.
- faster than the currently available fission track detection software (to our knowledge).
- reliable and robust because it is not really sensitive to changes in optical settings.
- useful since it is software in which other, potentially smarter deep neural networks can be implemented.



## 150 **Code availability**

The presented software will be made available for academic research. The only requirement is to register by sending an e-mail to [Simon.Nachtergaele@UGent.be](mailto:Simon.Nachtergaele@UGent.be) in order to obtain a password. Then, software can be downloaded for free at <https://users.ugent.be/~smanacht/download.html>.

## **Video supplement**

155 Tutorial AI-Track-tive: <https://www.youtube.com/watch?v=fSfit87vkrA&t=1s>

## **Author contribution**

SN conceptualized the implementation of computer vision techniques for fission track detection and trained the deep neural networks. SN wrote the software and performed all experiments described in this paper. SN made the tutorial video that can be found in video supplement. JDG acquired funding for the fission track microscope system and reviewed the manuscript.

## 160 **Competing interest**

The authors declare that they have no conflict of interest.

## **Acknowledgments**

SN is very grateful for the PhD scholarship received from FWO (Research Foundation Flanders). Kurt Blom is thanked for explanations on software security.

## 165 **References**

Belloni, F. F., Keskes, N. and Hurford, A. J.: Strategy for fission-track recognition via digital image processing, and computer-assisted track measurement, in 9th International Conference on Fission-Track Dating and Thermochronology: Geological Society of Australia Abstracts, pp. 15–17., 2000.

Bradski, G.: The OpenCV Library, Dr Dobbs J. Softw. Tools, 25, 120–125, doi:10.1111/0023-8333.50.s1.10, 2000.

170 Enkelmann, E., Ehlers, T. A., Buck, G. and Schatz, A. K.: Advantages and challenges of automated apatite fission track

counting, *Chem. Geol.*, 322–323, 278–289, doi:10.1016/j.chemgeo.2012.07.013, 2012.

Fleischer, R. L., Price, P. B. and Walker, R. M.: Nuclear tracks in solids: principles and applications, University of California Press., 1975.

175 Gleadow, A. J. W., Duddy, I. R., Green, P. F. and Lovering, J. F.: Confined fission track lengths in apatite: a diagnostic tool for thermal history analysis, *Contrib. to Mineral. Petrol.*, 94(4), 405–415, doi:10.1007/BF00376334, 1986.

Gleadow, A. J. W., Gleadow, S. J., Belton, D. X., Kohn, B. P., Krochmal, M. S. and Brown, R. W.: Coincidence mapping - A key strategy for the automatic counting of fission tracks in natural minerals, *Geol. Soc. Spec. Publ.*, 324(September), 25–36, doi:10.1144/SP324.2, 2009.

180 Gold, R., Roberts, J. H., Preston, C. C., Mcneece, J. P. and Ruddy, F. H.: The status of automated nuclear scanning systems, *Nucl. Tracks Radiat. Meas.*, 8, 187–197, 1984.

Hurford, A. J. and Green, P. F.: The zeta age calibration of fission-track dating, *Chem. Geol.*, 41, 285–317, doi:10.1016/S0009-2541(83)80026-6, 1983.

Jonckheere, R.: On the densities of etchable fission tracks in a mineral and co-irradiated external detector with reference to fission-track dating of minerals, *Chem. Geol.*, 41–58, doi:10.1016/S0009-2541(03)00116-5, 2003.

185 Kumar, R.: Machine learning applied to autonomous identification of fission tracks in apatite, *Goldschmidt2015 Abstr.*, 2015, 2015.

Lundh, F.: An Introduction to Tkinter, *Rev. Lit. Arts Am.*, (c), 166, 1999.

Malusà, M. G. and Fitzgerald, P.: *Fission-Track Thermochronology and its Application to Geology*, edited by M. G. Malusà and P. Fitzgerald, Springer International Publishing., 2019.

190 Petford, N., Miller, J. A. and Briggs, J.: The automated counting of fission tracks in an external detector by image analysis, *Comput. Geosci.*, 19(4), 585–591, 1993.

Van Ranst, G., Baert, P., Fernandes, A. C. and De Grave, J.: Technical note: Nikon – TRACKFlow, a new versatile microscope system for fission track analysis, *Geochronology*, 2(1), 93–99, 2020.

195 Redmon, J. and Farhadi, A.: YOLOv3: An Incremental Improvement, *ArXiv [online]* Available from: <http://arxiv.org/abs/1804.02767>, 2018.

Redmon, J., Divvala, S., Girshick, R. and Farhadi, A.: You Only Look Once: Unified, Real-Time Object Detection, *Proc. IEEE Conf. Comput. Vis. pattern Recognit.*, 779–788, 2016.

Van Rossum, G. and Drake Jr, F. L.: *Python reference manual*, Amsterdam., 1995.

de Siqueira, A. F., Nakasuga, W. M., Guedes, S. and Ratschbacher, L.: Segmentation of nearly isotropic overlapped tracks in



200 photomicrographs using successive erosions as watershed markers, *Microsc. Res. Tech.*, 82(10), 1706–1719, doi:10.1002/jemt.23336, 2019.

Wagner, G. A.: Archaeological applications of fission-track dating, *Nucl. Track Detect.*, 2(1), 51–63, doi:10.1016/0145-224X(78)90005-4, 1978.

Wagner, G. A. and Van den haute, P.: *Fission-Track dating*, Kluwer Academic Publishers, Dordrecht., 1992.

205

## Figures

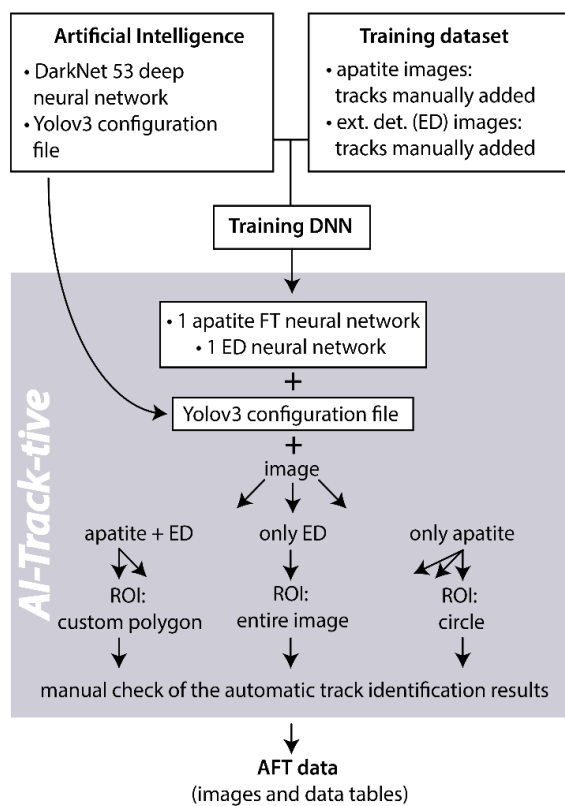
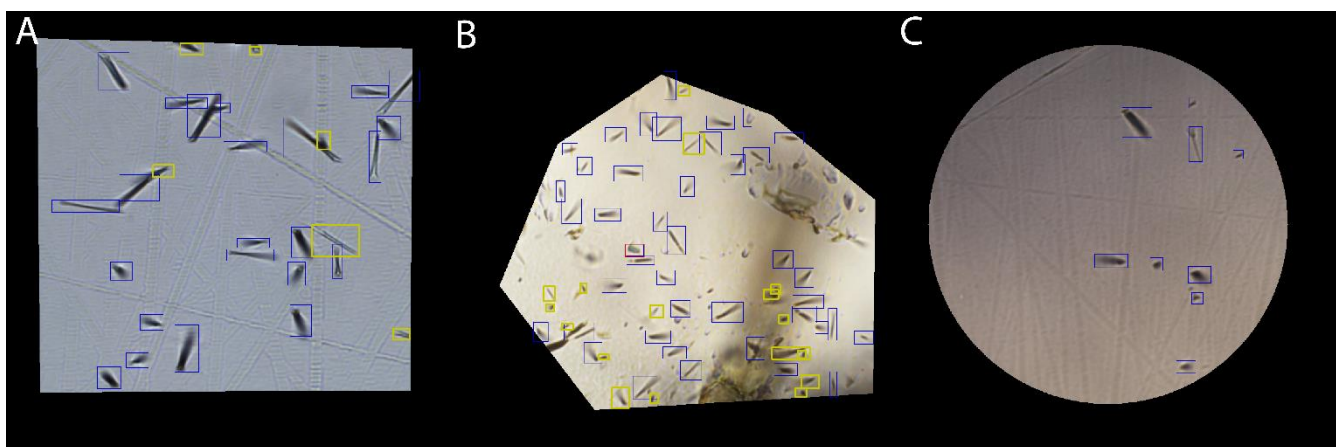


Figure 1: Flow chart of AI-Track-tive



210

215

Figure 2: fission track recognition results in apatite (scale: image is 100 μm on 100 μm) of AI-Track-tive. Panel A shows a pre-annealed Durango apatite (A-DUR) in which 23 out of 29 tracks were found automatically (success rate = 79%). Panel B shows a sample with a track density of  $1.26 \times 10^6$  tracks/cm<sup>2</sup> in which only 43 out of 59 tracks (73% success rate) were found and 1 was mistakenly added by the computer vision track identifier. Panel A and B show a custom-chosen polygonal counting window and panel C shows a circular window of 80 μm diameter on a Durango apatite in which all tracks were found automatically.

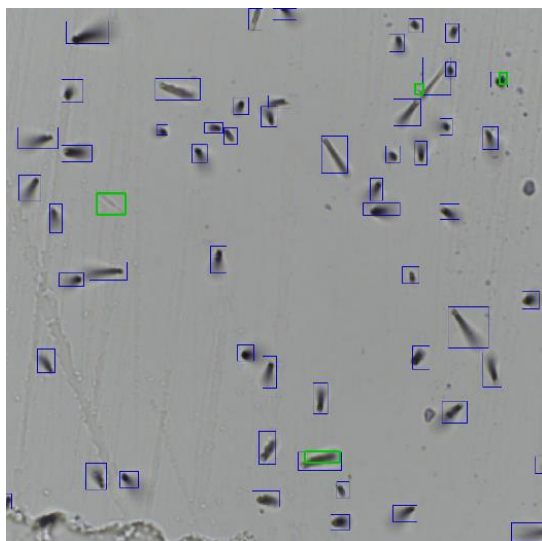
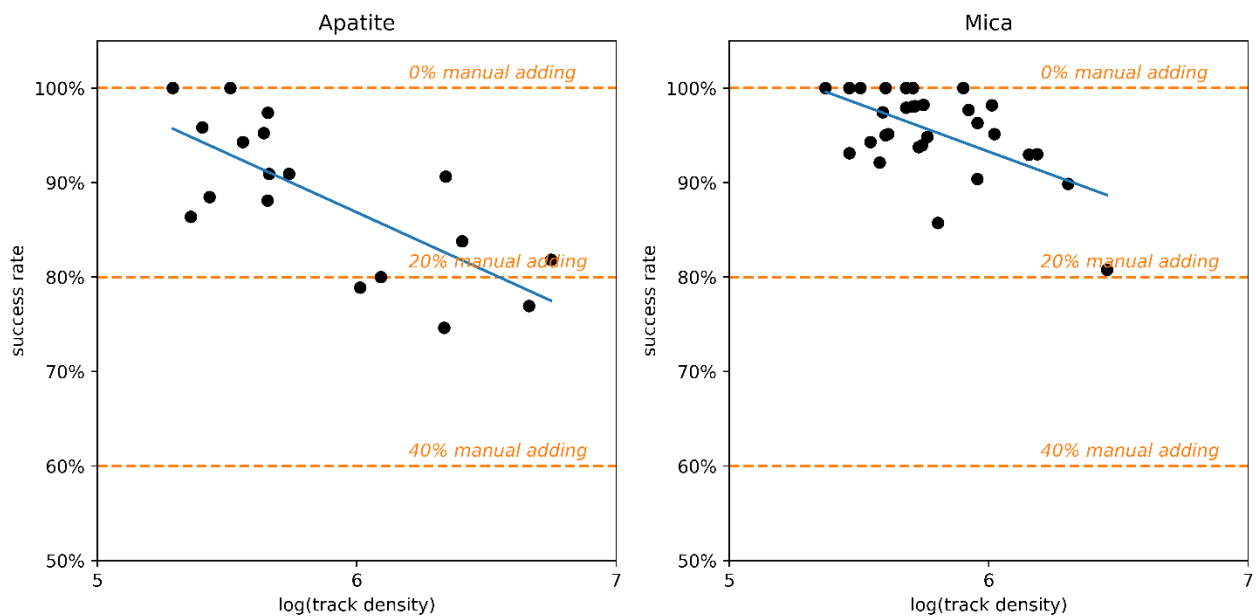


Figure 3: fission track recognition in muscovite (external detector).



220 **Figure 4: Results of the automatic track counting approach of our current deep neural network models for both apatite (left) and mica (right). The success rate of the automatic fission track recognition deep neural network is shown on the vertical axis. The 10-based log of areal track density (tracks/cm<sup>2</sup>) is shown on the horizontal axis.**



## Tables

225

**Table 1: results of the automatic fission track recognition in apatite. Areal track density ( $\rho$ ) is expressed in tracks/cm<sup>2</sup>. The number of automatically and manually detected tracks is indicated by  $n_{\text{auto}}$  and  $n_{\text{manual}}$ , respectively.**

<i>Apatite sample</i>	<i>Area</i> ( $\mu\text{m}^2$ )	$\rho$ (tracks/cm <sup>2</sup> )	$n_{\text{auto}}$	$n_{\text{manual}}$	<i>success rate</i>
A-DUR-G1_Ap_XY001_Z06_RGB.jpg	9602	4.37E+05	40	2	95%
A-DUR-G1_Ap_XY022_Z06_RGB.jpg	9625	3.64E+05	33	2	94%
A-DUR-G1_Ap_XY067_Z06_RGB.jpg	9272	4.53E+05	37	5	88%
A-DUR-G1_Ap_XY091_Z06_RGB.jpg	7187	4.59E+05	30	3	91%
BC-04_Ap_XY09_Z04_RGB.jpg	4358	2.20E+06	87	9	91%
BC-04_Ap_XY11_Z04_RGB.jpg	8376	4.54E+05	37	1	97%
BC-04_Ap_XY12_Z04_RGB.jpg	2904	2.55E+06	62	12	84%
BC-04_Ap_XY13_Z04_RGB.jpg	8025	5.48E+05	40	4	91%
BC-04_Ap_XY16_Z04_RGB.jpg	1373	5.61E+06	63	14	82%
BC-04_Ap_XY18_Z04_RGB.jpg	1409	4.61E+06	50	15	77%
BC-04_Ap_XY19_Z04_RGB.jpg	3085	2.17E+06	50	17	75%
BC-04_Ap_XY21_Z04_RGB.jpg	6889	1.03E+06	56	15	79%
BC-04_Ap_XY24_Z04_RGB.jpg	3636	1.24E+06	36	9	80%
DUR-G2_Ap-Lc_XY03_Z04_RGB.jpg	9602	2.29E+05	19	3	86%
DUR-G2_Ap-Lc_XY06_Z06_RGB.jpg	9463	2.54E+05	23	1	96%
DUR-G2_Ap-Lc_XY07_Z04_RGB.jpg	9524	3.25E+05	31	0	100%
DUR-G2_Ap-Lc_XY30_Z04_RGB.jpg	9609	2.71E+05	23	3	88%
DUR-G2_Ap-Uc_XY24_Z05_RGB.jpg	9224	1.95E+05	18	0	100%

**Table 2: results of the automatic fission track recognition in muscovite (external detector). Areal track density ( $\rho$ ) is expressed in tracks/cm<sup>2</sup>. The number of automatically and manually detected tracks is indicated by  $n_{\text{auto}}$  and  $n_{\text{manual}}$ , respectively.**

<i>Muscovite sample</i>	<i>Area</i> ( $\mu\text{m}^2$ )	$\rho$ (tracks/cm <sup>2</sup> )	$n_{\text{auto}}$	$n_{\text{manual}}$	<i>Success rate</i>
A-DUR-G1_EDr_XY015_Z6_RGB.jpg	10000	3.50E+05	33	2	94%
A-DUR-G1_EDr_XY016_Z6_RGB.jpg	10000	3.20E+05	32	0	100%
A-DUR-G1_EDr_XY017_Z6_RGB.jpg	10000	4.00E+05	38	2	95%
A-DUR-G1_EDr_XY018_Z6_RGB.jpg	10000	3.90E+05	38	1	97%
A-DUR-G1_EDr_XY019_Z6_RGB.jpg	10000	4.10E+05	39	2	95%
A-DUR-G1_EDr_XY020_Z6_RGB.jpg	10000	2.90E+05	27	2	93%
GL09_XY1_Z4_RGB.jpg	10000	2.90E+05	29	0	100%
GL09_XY2_Z4_RGB.jpg	10000	4.80E+05	47	1	98%
GL09_XY3_Z4_RGB.jpg	10000	5.60E+05	55	1	98%
GL09_XY4_Z4_RGB.jpg	10000	5.20E+05	51	1	98%
GL09_XY5_Z4_RGB.jpg	10000	5.20E+05	51	1	98%
GL09_XY6_Z4_RGB.jpg	10000	3.90E+05	38	1	97%
GL09_XY7_Z4_RGB.jpg	10000	3.80E+05	35	3	92%
GL09_XY8_Z4_RGB.jpg	10000	4.00E+05	40	0	100%
GL09_XY9_Z4_RGB.jpg	10000	5.10E+05	51	0	100%
GL09_XY10_Z4_RGB.jpg	10000	5.10E+05	50	1	98%
FCT-G4_EDr_XY002_Z4_RGB.jpg	5973	5.52E+05	31	2	94%
FCT-G4_EDr_XY005_Z4_RGB.jpg	9181	9.04E+05	75	8	90%
FCT-G4_EDr_XY007_Z4_RGB.jpg	6143	7.98E+05	49	0	100%
FCT-G4_EDr_XY011_Z4_RGB.jpg	5953	5.38E+05	30	2	94%
FCT-G4_EDr_XY033_Z5_RGB.jpg	7798	1.05E+06	78	4	95%
FCT-G4_EDr_XY048_Z5_RGB.jpg	3295	6.37E+05	18	3	86%
DUR-G2_EDr-Uc_XY04_Z2_RGB.jpg	10000	4.80E+05	48	0	100%
DUR-G2_EDr-Uc_XY12_Z3_RGB.jpg	10000	5.80E+05	55	3	95%
MY-2xyz01	5349	1.03E+06	54	1	98%
MY-2xyz14	4969	1.43E+06	66	5	93%
MY-2xyz17	6498	1.54E+06	93	7	93%



MY-2xyz27	3408	2.02E+06	62	7	90%
MY-2xyz29	4687	2.35E+05	11	0	100%
MY-2xyz33	5146	8.36E+05	42	1	98%
MY-2xyz39	3638	2.86E+06	84	20	81%
MY-2xyz40	5966	9.05E+05	52	2	96%

230

**Table 3: estimated time for 20-30 grains/polygons using different automated track recognition software packages and manual counting results from Enkelmann et al. (2012)**

	<i>Type</i>	<i>Alignment (min)</i>	<i>Grain selection + imaging (min)</i>	<i>Counting (min)</i>	<i>Analysis/computer conversion (min)</i>	<i>Total time (min)</i>
Enkelmann et al. (2012)	Analyst 1 FastTracks (Enkelmann et al. 2012)	20	40-60	180-240	40-90	240-410
	Analyst 2 FastTracks (Enkelmann et al. 2012)	20-30	30-60	120-240	90-180	260-510
	Manual (sandwich technique, analyst 1)	10	-	30-45	20 (digitizing data)	60-75
	Manual (sandwich technique, analyst 2)	5-15	-	30-90	20 (digitizing data)	55-125
This paper	AI-Track-tive (Durango sample)	10-20	25-35	30	5	70-90